Compression and creep of Venice Lagoon sands

Sanzeni A., Whittle A.J., Germaine J.T., Colleselli F.

Abstract

A laboratory test program has been conducted to evaluate the 1-D compression and creep properties of intact sand (and silty-sand) samples from a deep borehole at the Malamocco Inlet to the Venice Lagoon. The tests were performed with a CRS consolidometer and include special procedures for trimming the frozen samples, and measuring strains during thawing and back-pressure saturation. The specimens have variable fine fractions ranging from 6 to 21% and mica contents ranging from 1 to 10%. The results confirm that there is a strong correlation between the creep rate coefficient and the compressibility index, and between the swelling index and mica content. The compression behavior in all tests is well described by the model proposed by Pestana and Whittle (1995) with a unique Limiting Compression Curve and a variable transition parameter that reflects the fines and mica content. Creep tests performed at different confining pressures are also well represented by a simple two-parameter model.

Introduction

The economic dislocation and structural damage caused by frequent high tides in the city of Venice ("acqua alta", 99 events occurred in 1996) and potential destruction of the fragile surrounding lagoon environment by sea storm surges have led to the design of an extensive flood protection system currently under construction by the Consorzio Venezia Nuova (Harleman et al., 1996; http://www.consorziovenezianuova.com/). The centerpiece of this system is a set of mobile barriers (the "MOSE" system, acronym of "Electromechanic Sperimental MOdule") across the three inlets connecting the lagoon to the Adriatic Sea (Lido, Malamocco, and Chioggia). Each barrier consists of a row of concrete caissons supporting hinged hollow steel

gates that are normally filled with water and lie retracted on the seabed (at depths up to 20m). The gates are raised for tides exceeding 1.1m by injecting compressed air, and provide protection for surges up to 3.0m above mean sea level.

Since the 1970's there have been extensive studies of the subsurface soil conditions in the lagoon in order to understand and predict the causes of subsidence (Ricceri and Butterfield, 1974). More recently the geotechnical investigations have focused on the foundation conditions at the three inlets (Ministero dei Lavori Pubblici, 1994; Ricceri, 1997). The lagoon subsoil deposits comprise a complex system of interbedded sand, silt and silty clay sediments. While all of these materials are derived from the same parent Alpine (igneous and metamorphic) rocks, their accumulation took place in variety of depositional environments associated with the alternation of marine regressions and transgressions. Belloni and Caielli (1997) have given detailed accounts of the geological history of conditions at the Malamocco Inlet, where the soil profile comprises more than 75m of Holocene and late Pleistocene deposits formed in either coastal alluvial or shallow marine environments. Cola and Simonini (2002) have carried out extensive laboratory testing on these materials. They show that although the sediments have a unique geological origin, the profile is highly heterogeneous comprising 'chaotically interbedded' units of silts with variable clay and sand fractions (95% of these sediments can be classified as ML, CL or SP-SM materials in the USCS classification system). Various attempts have been made to provide a unified framework for interpreting the engineering properties of these materials. For example, Cola and Simonini (2002) report some success in correlating compression and small strain stiffness parameters to an empirical "grain size index". More recently Biscontin et al. (2007) have proposed a unifying framework for interpreting compression properties based on the gravimetric clay fraction (FF, $d < 5\mu m$) and estimates of

reference void ratios for the clay-water and granular (i.e., silt-sand) fractions (e_{c1V} and e_{g1V}, respectively).

While most of the prior studies on the lagoonal sediments have focused on the clay and silt units, the current paper deals exclusively with the sandy units, most of which are classified as poorly graded sands with silt (SP-SM and SM materials that account for approximately 35% of the sediments). An experimental test program has been conducted on samples obtained from an offshore boring (S5M by Consorzio Venezia Nuova, 2004) at the Malamocco inlet at depths ranging from 25–70m below mean sea level (the mudline is 16.8m b.m.s.l.). The samples were obtained using an Osterberg fixed-piston sampler and were frozen after recovery and shipped in dry ice to avoid densification and disturbance during transportation and handling (these procedures were selected by the contractor before the Authors' involvement). This paper describes measurements of 1-D compression and creep properties from a program of tests (on intact and reconstituted specimens) in a computer-controlled consolidometer device. In the course of this work, novel trimming procedures have been developed to prepare intact test specimens from the frozen samples (Sanzeni et al., 2007), together with a new method for estimating the content of micaceous material. Results of the tests are interpreted using the compression and creep models proposed for sands by Pestana and Whittle (1995, 1998).

Test Materials

Figure 1 shows an interpreted cross-section of the soil stratigraphy beneath the Malamocco inlet. The current test program has been performed on specimens obtained from six tube samples in boring S5M, two from the upper Holocene units (R and T at depths 25-28m b.m.s.l.) and four from the Pleistocene units (V1, E2, F2 and G2, with depths from 46-66m

b.m.s.l.). Previous studies on these sandy materials (Cola and Simonini, 2002) have found D_{50} = 0.07-0.3mm, with coefficient of uniformity, C_u = 1.5-3.5, and a mean roundness index R = 0.23-0.34, corresponding to angular or sub-angular grains.

The current study included basic classification tests (on trimmings for the test specimens) to determine the fines content and amount of micaceous material within the coarse fraction. The fines content was identified as the percentage of material passing through no. 200 sieve (0.075mm; ASTM Standard D422-63). There are no standard procedures for measuring the mica content. Instead, a simple technique was used to separate the flat mica particles on an inclined paper surface (Sanzeni, 2006). The surface roughness of standard printer paper is sufficient to trap most mica particles, while other sand grains roll off. Figure 2 illustrates the effectiveness of this process in separating flat mica particles (individual flakes have typical width of 0.3mm, Figure 2a) from the coarse sand fraction (Figure 2b). Although the method does not achieve a precise measure of the mica fraction, it is sufficient for basic classification and is well-suited for small samples (typical measurements were made on 10g of trimmings). Figure 1 summarizes the fines fraction and mica content measured from the tube samples. The fines content (silt and clay) ranges from 7-20%. Two of the tubes (R and V1) have very low mica content (1.2-2.4%), while the others have significantly larger fractions in the range 4-10%. Cola and Simonini (2002) found significant differences in the mineralogy of sandy materials from the Malamocco test site and recommended a basic sub-division between: i) carbonatic units (generally more prevalent at greater depths in the Pleistocene), with dolomite and calcite as the principal minerals; and ii) siliceous units where quartz and feldspar are dominant. They report larger fines fractions in the carbonatic units (typically up to 8% silt) while siliceous units contained less than 2% fines. No mineralogical studies were undertaken in the current study. However, there are notably higher

fractions of fines in the tube samples from S5M, while the mica content appears quite erratic. Figure 3 shows selected results of microscope mineralogical analyses performed in 2005 (Fontolan, 2005) on a number of samples from boring CH1M, drilled approximately 350m N-N-East of boring S5M, on the opposite side of the Malamocco inlet (Figure 1). Test were conducted on the 125-250μm fraction and results indicate that quartz is predominant in the Holocene unit (60-90%) and the mica fraction appears quite erratic (0-20%). In the Pleistocene deposits the amount of quartz grains is 40-70% and dolomite content is 15-60%, mica grains are almost non existent down to 70m b.m.s.l. and then significantly increasing although still irregular.

Experimental Program

Preparation of Intact Specimens

A program of 1-D compression tests have been carried out on intact specimens of the silty sands in a computer-controlled Constant Rate of Strain (CRS) consolidometer apparatus. The device is based on the original design by Wissa et al. (1971) and includes a base pore pressure transducer and conventional load cell, displacements are measured by an LVDT, and closed-feedback control is used to compensate for apparatus compressibility. The majority of the test program has been performed on intact specimens that were selected from radiographic images of the tube samples and trimmed directly to fit into the (60mm diameter, 25mm high) confining ring of the CRS cell. Although there is a considerable body of literature describing techniques for trimming frozen granular soils (Baker, 1976; Yoshimi et al., 1978; Goto, 1993; Okamura et al., 2003), none of these methods are suitable for 1-D compression testing where dimensional tolerances are particularly critical, as the soil specimen must fit tightly into the consolidometer ring. Sanzeni et al. (2007) have described a new method for trimming specimens

of frozen sand using a heated blade to shave soil from the outer surface of the specimen while concurrently advancing the sharp edge of the confining ring. The top and bottom surfaces of the specimens were kept frozen using dry ice packs, such that the trimming operation could be performed at room temperature. The intact (frozen) specimens were then allowed to thaw (and equilibrate) within the CRS apparatus at a fluid chamber pressure, σ_c = 100kPa and vertical total stress, σ_v = 110kPa, while measuring the vertical strain. Thereafter the cell pressure (now equivalent to the back-pressure of the thawed specimen) was increased to 400kPa and the vertical load adjusted to maintain a vertical effective stress σ'_v = 10kPa for 3 hours prior to performing the prescribed compression test.

Table 1 summarizes the program of compression tests performed on intact specimens together with pertinent drained compression and creep properties. It is important to note that there are large variations of the initial void ratios (e_0 in the frozen state) within given tube samples. A smaller set of tests was also performed on reconstituted specimens (using material from tube T, 27m b.m.s.l., Fig. 1). These were prepared by moist tamping in three layers to a target void ratio (using a fixed amount of solids with known water content).

Thawing Strains

Table 1 shows that significant vertical strains were measured after thawing and back-pressure saturation of the intact test specimens (in the range, $\Delta\varepsilon_T \approx 0.67\text{-}5.50\%$). The most likely cause of these strains is the procedure used to freeze tube samples. Figure 4a compares the initial void ratios of the frozen and thawed specimens (e_0, e_1, respectively) and Figure 4b relates the thawing strains with the specimen fines content. In the ideal case (A, Fig. 4a), there is free drainage within the tube sample during freezing such that water is expelled and there is no

volumetric expansion (or change in void ratio). The frozen and thawed void ratios should then remain equal ($e_0/e_1 = 1.0$). In contrast, case B represents the situation where there is no drainage of excess water within the fully saturated sand sample and there is a volumetric expansion of 9% as the water freezes. In this case, it is reasonable to expect the $e_1/e_0 \approx 0.91$ (assuming reversibility of expansion-contraction process).

Figure 4a shows that measured data generally lie within these two limits but most of the tests are closer to case B, indicating that probable volumetric expansion during freezing (this analysis assumes the expansion-contraction process is reversible). The reasons for the measured volume changes are uncertain, given the lack of information on the conditions under which the samples were handled and frozen. Expansion and subsequent thawing strain may be related to insufficient drainage of pore water and/or the presence of fines (Figure 4b), a factor that has the greatest effect on the quality of frozen sand samples (Yoshimi et al., 1978; Walberg, 1978; Seed et al., 1982; Goto, 1993). An alternative reason for the thaw strains could be over-cutting of the specimen during preparation, but this seems more unlikely as the test procedure achieved a tight fit inside the confining ring. It can be shown that the specimen would need to be over-cut by 1mm over the entire lateral surface (corresponding to 1.6% volume strain) in order to explain the measured thawing strain.

Compression Test Procedures

Most of the tests followed a standard procedure comprising: 1) one-dimensional compression at a prescribed strain rate, $\dot{\varepsilon} = 1.0\%$/hr to a maximum vertical effective stress, $\sigma'_{vm} = 2.0$MPa; 2) drained creep for a period of 24hrs at the maximum stress; and 3) unloading at $\dot{\varepsilon} = -0.5\%$/hr. Table 1 lists variations on this procedure that were used to evaluate effects of strain

rate, creep properties at different compression stress levels (multi-stage creep tests) etc.

Results

Figure 5a summarizes the typical compression behavior of intact and reconstituted silty sand specimens in a conventional e-logσ'_v space. The non-linear compression behavior depends on both the effective stress and void ratio of the specimens. This is most clearly seen by deriving the 1-D confined (tangent) modulus, M, from the data. Figure 5b shows that individual tests can be represented as power law functions of the effective stress, with a reference modulus ratio, c_1, (i.e., M/p_{at} defined at $\sigma'_v/p_{at} = 1$, where p_{at} is the atmospheric pressure) and exponent, m. The results show significant variations in both c_1 and m, for specimens within the same tube sample (e.g., #694 vs #695 in tube R), for intact versus reconstituted material (#726 vs #705, with similar fines fraction and mica content), and for upper and lower sand units (Holocene tube R vs Pleistocene tube E2 and F2). Alternatively, the compression index, C_c, can be interpreted directly from the conventional e-logσ'_v behavior (Fig. 5a). Values of C_c (at σ'_v = 2MPa, Table 1) are 0.067-0.118 for intact specimens of sample R (25.8-26.4m b.m.s.l., Holocene) and are generally higher than 0.140 for V1, E2, F2 specimens (46.7, 61.5, 62.1 m b.m.s.l. respectively, Pleistocene); the compression index of reconstituted specimens is 0.128-0.138 (sample T, 27.0-26.6 m b.m.s.l.).

Very small strains were recovered during the unloading phase of the tests. Table 1 shows that recoverable strains in the upper sand unit (tube R), $\Delta\varepsilon_U \approx 0.32\%$ are less than 10% of the compressive strains in primary loading (and smaller than the preceding 12hr creep strains); while data from the lower sands range from $\Delta\varepsilon_U = 0.9 - 1.2\%$. Several authors have postulated that the bridging action of platy-shaped mica particles acting across the smaller sand grains should

generate larger recoverable deformations (Gilboy, 1928; Hight et al., 1999). Figure 6 shows a tentative linear correlation between the swelling index, C_s, and the mica content. This result appears to describe quite well the measured data for all of the specimens (including the reconstituted material) with the noted exception of V1 (where C_s is much higher than expected from the low mica content).

Creep properties of the silty sands have been measured in most of the tests at σ'_v = 2MPa over periods of 12-24hrs, and at a range of stress levels (σ'_v = 0.03-2MPa) in multi-stage tests (specimens #697, 701 and 704; Table 1). For intact specimens, the creep strains measured over a 24hr period at 2MPa range from $\Delta\varepsilon_S$ = 0.32-0.61%, while smaller strains were found for the reconstituted specimens ($\Delta\varepsilon_S$ = 0.23-0.34%). According to Mesri and Castro (1987) the coefficient of secondary compression, $C_{\alpha e}$, is proportional to the compression index C_c. Recent data by Mesri and Vardhanabhuti (2009) show $C_{\alpha e}/ C_c$ = 0.015-0.030 for a wide range of sands. In comparison, Figure 7 shows slightly higher ratios of secondary to primary compression, $C_{\alpha e}/ C_c$ = 0.034 and 0.030 for the upper Holocene and lower Pleistocene units respectively. However, the reconstituted specimens are more consistent with the empirical database ($C_{\alpha e}/ C_c$ = 0.022). The ratio $C_{\alpha e}/ C_c$ is not well correlated with either the fine content and/or mica fraction.

Model Framework

Pestana and Whittle (1995) proposed a non-linear compression model for freshly deposited cohesionless soils that assumes that specimens loaded from different formation densities approach a unique response at high stresses. This Limiting Compression Curve, LCC, is characterized by a linear relationship in $\log(e) - \log(\sigma'_v)$ space:

$$\log(e) = -\rho_c \left(\frac{\sigma'_v}{\sigma'_{vr}} \right) \tag{1}$$

where ρ_c is the compressibility index and σ'_{vr} is the reference effective stress at unit void ratio (e = 1.0). The incremental vertical effective-stress strain behavior during 1-D compression is described by:

$$d\varepsilon_v = \frac{e}{1+e} \left\{ \underbrace{\frac{\tilde{K}}{C_b} \left(\frac{\sigma'_v}{p_a} \right)^{-1/3} \delta_b^{\theta}}_{Elastic} + \underbrace{\rho_c \left(\frac{\sigma'_v}{p_a} \right)^{-1} \left(1 - \delta_b^{\theta} \right)}_{Plastic} \right\} \frac{d\sigma'_v}{p_a} \tag{2a}$$

$$\delta_b = 1 - \frac{\sigma'_v}{\sigma'_{vr}} (e)^{1/\rho_c} \tag{2b}$$

where p_a is the atmospheric pressure, $\tilde{K}$ is a parameter that expresses the variation in K_0 during 1-D compression (typically in the range 0.7–1.0; in the absence of K_0 measurements, the current analyses assume $\tilde{K}$ = 1.0), and C_b is a material constant that controls the small strain elastic stiffness.

Equation 2a expresses the total strain as weighted average of elastic and plastic strain components through a stress ratio, δ_b, that defines proximity of the current stress state to an equivalent stress on the LCC line (at the same void ratio). The constant exponent, θ, describes the elasto-plastic transition associated with the onset and progression of particle crushing.

The complete compression model (Eqn. 2) requires 4 input parameters (σ'_{vr}, ρ_c, θ and C_b), and must be integrated numerically. Pestana and Whittle (1995) also suggested a simplified analytical model for cases where: 1) elastic strains are negligible; and 2) the imposed stress range is much less than that needed to reach LCC conditions ($\delta_b << 1$). These assumptions lead to a linear relation between $\log_e(e/e_0)$ and vertical effective stress:

$$\log_e\left(\frac{e}{e_0}\right)=-\left(e_0\right)^{1/\rho_c}\beta\left(\frac{\sigma'_v}{p_a}\right) \tag{3a}$$

$$\beta=\rho_c\theta/(\sigma'_{vr}/p_a) \tag{3b}$$

where e_0 is the initial void ratio.

Pestana and Whittle (1998) proposed a simple extension of the compression model to account for time dependent creep deformations. The LCC regime is characterized by parallel isochronous compression lines, which are analogous to the secondary compression models for cohesive soils:

$$\log\left(e\right)=-\rho_c\log\left(\frac{\sigma'_v}{\sigma'_{vr}\left(t_{ref}\right)}\right)-\rho_\alpha\left(\frac{t}{t_{ref}}\right) \tag{4}$$

where ρ_α is a creep rate coefficient that characterizes the rate of deformation at constant vertical effective stress in the LCC regime, and t_{ref} is a reference time.

The incremental effective stress-strain-time relations during 1-D compression can then be computed using a transformed stress ratio, δ_b, in Eqn. 2a:

$$\delta_b=1-\frac{\sigma'_v}{\sigma'_{vr}}\left(e\right)^{1/\rho_c}\left(\frac{t}{t_{ref}}\right)^{\rho_\alpha/\rho_c} \tag{5}$$

Compression Parameters

The selection of Venetian sand parameters was first approached using the simplified model formulation for low stresses (Eqn. 3a). The comparison between selected experimental data and Eqn. 3 is presented in Figure 8 and demonstrates the capability of the analytical solution to reproduce compression behavior of Venice Lagoon sand within the applied stresses. For Holocene specimens (R, 26.0 m b.m.s.l.), the parameter β was 0.006-0.009 with average value

0.007 adopted for subsequent interpretation. Higher values (β = 0.009-0.013) were found suitable for specimens from other Pleistocene samples (Table 1). The comparison in Figure 8 shows a discrepancy between measured and computed compression in the range 0.1-0.3 MPa and a difference between measured initial void ratio, e_0, and the corresponding selected value in the computed response. The authors believe that this difference is in relation with sample disturbance caused during freezing.

Small strain stiffness

According to Pestana and Whittle (1995), the parameter C_b can be inferred from measurements of shear wave velocity, V_s, with the following equations:

$$\left(G_{\max} / p_{at}\right) = C_b \frac{3}{2} \frac{(1-2\mu)}{(1+\mu)} \frac{1}{n} \left(\frac{p'}{p_a} \right)^{1/3} \tag{6a}$$

$$G_{\max} = \rho V_s^2 \tag{6b}$$

where p' is the mean effective stress, μ is the Poisson's ratio, n is the porosity, and ρ the unit weight of soil.

Eqn. 6 was applied to recent (unpublished) measurements of shear wave velocity, taken with a bender element system in the triaxial cell. Tests were performed independently of this study between 2004 and 2006 at ISMGeo laboratory (former ISMES Geotecnica; Bergamo, Italy) and were carried out on specimens of sand (SP and SP-SM), obtained from undisturbed samples retrieved from several boreholes at the Malamocco inlet to the Venetian lagoon (tests commissioned by the Consorzio Venezia Nuova, 2004-2006).

Measured values of $G_{\max} / p_a$ are reported in Figure 9 as a function of the normalized mean effective stress p' / p_a. Assuming μ = 0.20-0.23, the best fit of laboratory results was

achieved by Eqn. 6a with C_b = 600. The slope of Eqn. 6a in Figure 9 is primarily governed by the exponent 1/3, which was selected by Pestana and Whittle (1995) according to the Hertzian contact theory for elastic compression of spheres. The performance of Eqn. 6a was also compared with alternative empirical relationships recently developed to predict the value of maximum shear modulus, $G_{\max}$ (Pestana and Salvati, 2006; Biscontin et al., 2007; Figure 9). In general, a higher value of the exponent of p'/p_a provides a better fitting of data, particularly at low confining pressures.

LCC states

In Equation 1, the parameter ρ_c describes the slope of the LCC curve and can be unambiguously determined when compression tests to very high stresses are available. The level of stress reached in the CRS tests did not allow a direct estimation of the parameter and the value $\rho_c = 0.39$ was selected from considerations reported by Pestana and Whittle (1995) on previous modeling of sands.

The reference vertical stress at unit void ratio, σ'_{vr}, is used to locate the LCC in the $\log(e) - \log\sigma'_v$ space. Pestana and Whittle (1995) showed that particle size has a major effect on the parameter and proposed the following empirical correlation with mean particle size, D_{50}:

$$\sigma'_{vr}/p_a \approx \begin{cases} 15/D_{50}^{0.5}, & \text{angular particles} \\ 50/D_{50}^{0.5}, & \text{rounded particles} \end{cases} \qquad (7)$$

(also reported in Pestana et al., 2002), which can be used when compression tests to high stresses are not available. Venice Lagoon sand grains are angular to sub-angular, as observed by Belloni and Caielli (1997), hence Equation 7 gives average value σ'_{vr}/p_a = 20 ($\sim\sigma'_{vr}$ = 2.0MPa).

Biscontin et al. (2001, 2007) have also proposed LCC parameters for interpreting compression behavior of Venice Lagoon soils (classified as CL, ML and SP-SM). Biscontin et al. (2001) adopted a similar value, ρ_c = 0.40, based on oedometer tests (up to 5-6MPa) on 3 undisturbed specimens of SP-SM materials and 5 undisturbed specimens of ML materials (with fines content of 2.5-11.4%). More recently, Biscontin et al. (2007) examined reconstructed SP-SM specimens and proposed that a lower value, ρ_c = 0.24, could be adopted for the CL, ML and SP-SM soils.

Transition regime

The transition parameter, θ, describes the progressive breakage of particles as specimens are compressed into the LCC regime and can be directly determined from laboratory compression tests to relatively high pressures. In general, high values of θ are typical of a material with a more gradual transition to the LCC regime, while low values represent materials with well defined yield points associated with particle breakage (Nikolinakou et al., 2004). Pestana and Whittle (1995) showed that θ is affected by soil grading and can be expressed as a function of the Coefficient of Uniformity, C_u, and particle angularity. Pestana et al. (2002), proposed the following correlation:

$$\theta \approx 0.10 C_u + a \qquad (8)$$

with $a = 0.0,\ 0.05,\ 0.15,\ 0.25$ for rounded, subrounded, subangular and angular particles respectively. Assuming a = 0.20, C_u = 1.5-2.5 for Holocene sands (tube R) and C_u = 3.0-6.5 for Pleistocene materials, Eqn. 8 predicts θ = 0.35-0.70 depending on soil grading. This estimation is comparable with values proposed by Biscontin et al. (2007) for angular, sub-angular sands and

silty sands and is consistent with values of θ backfitted with Eqn. 3b using the herein proposed values of β and LCC parameters, ρ_c and σ'_{vr} / p_a.

Evaluation of Compression Model

The parameters C_b = 600, ρ_c = 0.39, σ_r / p_a = 20 and θ = 0.35-0.70 were adopted for describing compression response of Venice Lagoon sand. To evaluate model performance, a comparison was first made with experimental data obtained from tests on reconstituted specimens and a subsequent comparison was made between model predictions and measurements obtained from tests executed on intact specimens (Figure 10).

In general, the compression of Venice Lagoon sand is well described by the conceptual framework proposed by Pestana and Whittle (1995). However, the behavior of reconstituted and intact specimens could not be reproduced with a unique value of θ in the transition regime. In particular, θ = 0.60, found for reconstituted specimens (tube sample T, Fig. 10), was not applicable for all intact specimens. Figure 10 shows that model predictions were satisfactory when θ = 0.35 was adopted for specimens of tube sample R (25.8-26.4m below m.s.l.), but higher values (θ = 0.40-0.70) were required for matching measured response of specimens from higher depths in the stratigraphy. This evidence is consistent with observed variation of parameter β (Eqn. 3), and reflects the heterogeneity of soil grading and mineralogical composition. Table 1 reports parameters of transition parameter θ for each sample.

The comparison between measured and computed response of specimens prepared from frozen samples (Figure 10) showed a notable difference between experimental and predicted void ratio for stresses lower than σ' / p_a = 1. While the discrepancy was observed for most intact specimens, it was almost non-existent for remolded material. The authors believe that the

difference may be related with sample disturbance due to the presence of fines in the sand and insufficient drainage of pore water upon freezing.

Figure 10 also shows the LCC line recommended by Biscontin et al. (2007) (ρ_c = 0.24 and σ'_{vr} / p_a = 11.4). Their parameters are lower than values proposed in this paper and generally out of the ranges reported by Pestana and Whittle (1995) for a variety of natural and artificial sands. The effect of such a choice is to predict compression behavior characterized by LCC conditions occurring at lower stresses and lower compressibility at very high stresses.

Creep Parameters

The time-dependent behavior of Venice sand was studied by comparing Eqn. 4 with standard 24hr creep tests, carried out at constant stress level σ'_v = 2.0MPa on reconstituted and intact specimens, and selecting appropriate values of parameters t_{ref} and ρ_α. Figure 11 shows an example of calibration and the influence of model parameters on the numerical simulation, and Table 1 lists creep parameters selected for each sample. Creep behavior of intact test specimens of Venetian sand was well reproduced with t_{ref} = 0.1-0.2hr (9±3min) and a creep coefficient ρ_α = 0.0075±0.0015. However, tests conducted on reconstituted specimens were best fitted with lower ρ_α = 0.004 (consistent with values of the ratio $C_{\alpha e} / C_c$ in Fig. 7).

The selected creep parameters were used for computing time-dependent behavior of intact specimens undergoing creep at different stress levels (in the range 30-2000kPa), as shown in Figure 12. The comparison shows excellent agreement between model prediction and experimental data when values t_{ref} = 0.13hr and ρ_α = 0.006 are adopted, and demonstrates that the model extension is capable of predicting creep incremental strain as a function of the stress

level. Pestana and Whittle (1998) proposed sets of parameters to describe time effects on the compression response of mono-minerallic and natural sands (reconstituted soils). Although the number of granular materials presented was limited, the creep rate coefficient varied within a fairly narrow range (ρ_α = 0.0075-0.0150), while the reference time varied significantly, from 10 minutes, in the case of Ottawa Sand, up to 2 hours, for other sands. Venice Lagoon sand has similar creep rate ρ_α to Hostun Sand, a silica sand with comparable mean particle size and uniformity, but lower t_{ref} , meaning that secondary compression in Venice sand takes place earlier after the end of loading. A different behavior is seen for Ottawa Sand and Ground Quartz and t_{ref} = 10min was selected for both materials. However, it is important to note that Pestana and Whittle (1998) obtained their parameters from incremental 1-D and isotropic compression tests, while the current experimental results of this work were obtained from creep tests performed after CRS computer-controlled loading.

Conclusions

This paper reported on the compression and creep behavior of Venice Lagoon sand and silty sand. A number of samples were available from a boring carried out at the Malamocco inlet to the Lagoon. The study comprised an extensive laboratory investigation on intact (initially frozen) and reconstituted specimens, and the analysis of soil response in the light of an advanced compression model which includes time effects in the compression of sands (Pestana and Whittle, 1995, 1998). The main findings from study are as follows:

- Thawing strains measured on intact (initially frozen) specimens suggested that a volumetric expansion occurred during freezing. This behavior reflects unknown details of the sampling

process and may be affected by the fines content or insufficient drainage of pore water during freezing.

- Compression tests indicated a notable variability in the compression response that can be related with local variation of soil grading and mineralogical composition, even within the same sample. In general, sand specimens from the upper Holocene unit (sample R) were less compressible than specimens from the lower Pleistocene units. This is most likely related to changes in mineralogy and particle grading as reported by Cola and Simonini (2002).
- Very small strains were recovered during the unloading phase of the tests (in some cases less than 10% of the compressive strains in primary loading). Unloading response can be related to the platy-shaped mica particles whose presence contributes to increase the recoverable deformation. Tests on reconstituted specimens did not show any relevant difference with behavior observed for intact, initially frozen, materials and a tentative linear correlation between the swelling index and the mica content, was found to describe quite well the measured data for most specimens.
- Creep tests preformed at different stress levels demonstrated that time has significant influence on compression of Venetian sand. The creep strain rate parameter $C_{\alpha e}$ is highly correlated with the primary compression index Cc as proposed by Mesri and Castro (1987), with measured ratios $C_{\alpha e} / C_c$ = 0.034 and 0.030 for the upper Holocene and lower Pleistocene units respectively.
- Within the range of stresses explored in this study, the compression behavior of Venice Lagoon sand appeared to be described by the conceptual framework originally proposed by Pestana and Whittle (1995), using a fixed set of parameters for the Limiting Compression Curve (LCC, ρ_c = 0.39 and σ'_{vr} / p_a = 20) and a variable parameter θ to represent the

progression of particle crushing (affected by mineralogy and particle size distribution). The reported data show θ = 0.35-0.70 for the intact sand specimens, consistent with backfitting of parameter β in the low stress range.

- Creep tests performed at different confining pressures are well reproduced by the Pestana and Whittle (1998) model, with parameters t_{ref} = 0.1-0.2hr (9±3min) and ρ_α = 0.0075±0.0015.

Acknowledgments

This work was carried out through a collaborative project between the University of Brescia (Italy) and MIT. The authors wish to thank the Magistrato alle Acque and Consorzio Venezia Nuova for providing and shipping the soil samples and ISMgeo (Bergamo, Italy).

References

Baker T. H. W. (1976). “Preparation of Artificially Frozen Sand Specimens”, *Soil Specimen Preparation for Laboratory Testing*, ASTM STP 599, 88-112.

Belloni, L., and Caielli, A. (1997). “Origine dei Sedimenti a Malamocco.” Estratto dagli Atti dell’Istituto Veneto di Scienze, Lettere ed Arti, Tomo CLV (1996-1997) – Classe di Scienze Fisiche, Matematiche e Naturali (in Italian).

Biscontin, G., Pestana, J. M., Cola, S., Simonini, P. (2001). "Influence of grain size on the compressibility of Venice Lagoon soils." *Proc. XVth Int. Conf. Soil Mech. Found. Engng*, Istanbul, Turkey, Vol. IV, 2801-2804.

Biscontin, G., Cola, S., Pestana, J.M., Simonini, P. (2007). “Unified Compression Model for Venice Lagoon Natural Silts.” *J. Geotech. Geoenviron. Eng.*, Vol. 133(8), 932-942.

Cola, S., and Simonini, P. (2002). “Mechanical Behavior of Silty soils of the Venice Lagoon as a Function of their Grading Characteristics”, *Can. Geotech. J.*, 39, pp. 879-893.

Fontolan, G. (2005). “Analisi sedimentologiche (Op. 327-Conv. 7322) sondaggio CH1M – Rapporto conclusivo, Parte 1, Parte 2”. University of Trieste, DISGAM, commissioned by the Consorzio Venezia Nuova (in Italian).

Gilboy, G. (1928). “The compressibility of sand-mica mixtures.”, *ASCE Papers and Discussions*, 555-568.

Goto, S. (1993). “Influence of a freeze and Thaw Cycle on Liquefaction Resistance of Sandy Soils”, *Soils and Foundations*, Japanese Society of Soil Mechanics and Foundation Engineering, Tokyo, Japan, 33(4), 148-158.

Harleman, D. R. H., Bras, R. L., Rinaldo, A., Malanotte Rizzoli, P. (2000). “Blocking the Tide.”, *Civil Engineering* (N.Y.), 70(10), 52-57.

Hight, D. W. (1999). “Flow Slides in Micaceous Sands.”, *Problematic Soils*, Rotterdam, The Netherlands, ISBN 9054109971, 945-958.

Mesri, G., and Castro, A. (1987). “C_α/C_c Concept and K_0 during Secondary Compression.”, *J. Geotech. Eng.*, 113(3), 230-247.

Mesri, G. and Vardhanabhuti, B. (2009). “Compression of Granular Materials”, *Can. Geotech. J.*, 46, pp. 369-392.

Ministero dei Lavori Pubblici – Magistrato alle Acque (1994). “Nuovi Interventi per la Salvaguardia di Venezia. Interventi alle Bocche Lagunari.” Campagna di Indagini Geognostiche, Prove Geotecniche e Prove di Laboratorio. Bocca di Malamocco, Consorzio Venezia Nuova, Venezia, Italy (in Italian).

Okamura, M., Ishihara, M., Oshita, T. (2003) “Liquefaction Resistance of Sand Deposit Improved with Sand Compaction Piles.”, *Soils and Foundations*, Japanese Society of Soil Mechanics and Foundation Engineering, Tokyo, Japan, 43(5), 175-187.

Pestana, J. M., and Whittle, A. J. (1995) “Compression Model for cohesionless Soils”. Geotechnique 45, No. 4, pp. 611-631.

Pestana, J. M., and Whittle, A. J. (1998) “Time Effects in the Compression of Sands”. Geotechnique 48, No. 5, pp. 695-701.

Pestana, J. M., Whittle, A. J., Salvati, L. A. (2002). “Evaluation of a Constitutive Model for Clays and Sands; Part I – Sand Behavior.” *Int. J. Numer. Analyt. Meth. Geomech.*, 26, 1097-1121.

Pestana, J. M., and Salvati, L. A. (2006). “Small-Strain Behavior of Granular Soils. I: Model for Cemented and Uncemented Sands and Gravels.” *J. Geotech. Geoenviron. Eng.*, 132(8), 1071-1081.

Ricceri, G., and Butterfield, R. (1974). “An Analysis of Compressibility Data from a Deep Borehole in Venice.” *Géotechnique*, 24(2), 175-192.

Ricceri, G. (1997). "Geotechnical Problems for the Barriers." *Symposium on "Venice and Florence: a complex dialogue with water"*, ITCOLD, Comitato Nazionale Italiano Grandi Dighe, Patron, Bologna.

Sanzeni, A. (2006). "A Study on the Compression Behavior of Venice Lagoon Silty Sand." Ph.D. dissertation, Università degli Studi di Parma, Parma, Italy.

Sanzeni, A., Germaine, J. T., Whittle, A. J., Colleselli, F. (2007). "A Novel Trimming Technique for Frozen Sand Specimens." *Geotech. Testing J.*, ASTM, 30(6), 508-511.

Seed, H. B., Singh, S., Chan, C. K., Vilela, T. F. (1982). "Considerations in undisturbed sampling of sands". ASCE, *J. Geotech. Eng. Div.*, 108(GT2), 265-283.

Walberg, F. C. (1978). "Freezing and Cyclic Triaxial Behavior of Sands". ASCE, *J. Geotech. Eng. Div.*, 104(GT5), Proc. Paper 13722, 667-671.

Wissa, A. E. Z., Christian, J. T., Davis, E. H., Heiberg, S. (1971). "Consolidation at Constant Rate of Strain". ASCE, *J. Soil Mech. Foundation Div.*, 97(SM10), 1393-1413.

Yoshimi, Y., Hatanaka, M., Oh-oka, H., (1978). "Undisturbed sampling of saturated sands by Freezing." *Soils and Foundations*, 18(3), 59-73.

Sample Depth (m bmsl)	CRS Test	Soil Type	Fines [Mica]	Thawing		Compression-unloading					Creep		Model parameters[4]			
				e_0 [e_1]	$\Delta\varepsilon_T$ thaw	σ'_v	ε_v	C_c	C_s	$\Delta\varepsilon_u$ unload	$C_{\alpha e}$	$\Delta\varepsilon_s$ creep	β	θ	t_{ref}	ρ_α
			(%)	-	(%)	(kPa)	(%)	-	-	(%)	-	(%)	-	-	(hr)	-
R	694	SP-SM	6.7 [1.2]	0.738 [0.727]	0.63	2000	2.87	0.067	0.0026	0.322	0.0031	0.37[3]				
25.8-26.4	695	SP-SM	12.7 [1.3]	0.800 [0.781]	1.07	2000	4.03	0.080	0.0027	0.321	0.0032	0.48	0.007	0.35	0.10	0.008
	696	SP-SM	-	0.860 [0.785]	4.02	2000	5.48	0.100	0.0026	0.315	-	-				
	697	-	-	-	N/A	33	-	0.025	-	-	0.0007	0.09				
						112	-	0.036	-	-	0.0011	0.14				
						337	-	0.051	-	-	0.0015	0.22	0.007	0.35	0.13	0.006
						1125	-	0.089	-	-	0.0025	0.35				
						2250	6.60	0.134	-	-	0.0034	0.46				
	698	SP-SM	11.9 [1.4]	0.972 [0.864]	5.49	2000	6.05	0.117	0.0026	0.340	0.0045	0.58	0.007	0.35		
	699	SM	-	0.884 [0.789]	5.01	2000	6.55	0.118	-		0.0044	0.39	0.009	0.45	0.10	0.008
	700	SP-SM	8.8 [1.6]	0.894 [0.868]	1.34	2000	5.14	0.108	0.0035	0.402	0.0045	0.54	0.006	0.31		
	701	-	-	0.812 [0.765]	2.57	28	-	0.023	-	-	0.0005	0.08				
						97	-	0.030	-	-	0.0009	0.11				
						296	-	0.042	-	-	0.0015	0.20	0.008	0.40	0.13	0.006
						991	-	0.067	-	-	0.0026	0.34				
						1984	5.23	0.100	0.0024	0.303	0.0027	0.39				
T	702	SP-SM	-	0.923 [0.847]	3.54	1000	-	0.118	-		-	-	0.010	0.5	-	-
27.0-27.6	703	SM	12.8 [5.2]	0.942 [0.875]	3.41	2000	7.07	0.120	0.0076	0.911	0.0037	0.42	0.008	0.4	-	-
	704	SP-SM	10.8 [5.1]	1.020 [0.950]	3.63	32	-	0.022	-	-	0.0009	0.09				
						110	-	0.038	-	-	0.0014	0.16	-	-	0.13	0.008
						334	-	0.062	-	-	0.0016	0.20				
V1	722	SM	13.3 [2.4]	0.848 [0.791]	3.06	2000	7.71	0.156	0.0084	0.947	0.0055	0.57[3]	0.012	0.65	0.20	0.009
46.7-47.3	724	SM	13.6 [2.2]	0.833 [0.769]	3.48	2000	7.10	0.150	0.0083	0.943	0.0042	0.42[3]	0.013	0.70		
E2	726	SP-SM	9.7 [7.1]	0.879 [0.837]	2.24	2000	5.59	0.140	0.0084	-	0.0042	0.35[3]	0.008			
61.5-62.1	728	SP-SM	7.7 [10.0]	0.902 [0.846]	2.95	2000	6.56	0.170	-	-	0.0053	0.52	0.009	0.40	0.20	0.007
	729	SP-SM	-	0.915 [0.869]	2.40	2000	4.66	0.160	0.1030	1.227	0.0051	0.53	0.007			
F2	730	SP-SM	12.6 [7.6]	0.847 [0.800]	2.53	2000	5.08	0.129	0.0085	-	0.0037	0.43	0.009	0.50	0.13	0.006
62.1-62.7	731	SP-SM	11.4 [6.3]	0.831 [0.766]	3.60	2000	4.99	0.115	0.0080	0.925	0.0029	0.34	0.009			
G2	732	SM	14.9 [4.3]	0.812 [0.733]	4.40	2000	5.40	0.100	0.0064	-	0.0026	0.32	0.011	0.60	0.17	0.007
65.6-66.2	733	SM	21.3 [6.1]	0.992 [0.923]	3.46	2000	10.5	0.202	0.0084	0.983	0.0052	0.61	0.012			
	705			- [0.838]	-	2000	6.81	0.128	0.0054	-	0.0026	0.31	0.009			
T[1]	706			- [0.640]	-	2000	3.17	0.079	0.0046	0.687	0.0016	0.23	0.010			
27.0-27.6	707	SM-SP	14.0 [6.9]	- [0.843]	-	2000	6.50	0.137	0.0074	0.859	0.0027	0.28	0.009	0.60	0.15	0.004
	708			- [0.848]	-	2000	6.13	0.138	0.0069	0.836	0.0027	0.34	0.009			
	721[2]			- [0.842]	-	2000	5.34	0.132	-	-	0.0036	0.45	0.009			

[1]: reconstituted specimens; [2]: halved height specimen; [3]: 12hrs creep test; [4]: other model parameters C_b=600, ρ_c=0.39, σ'_r/p_{at}=20

Table 1. Relevant information on samples, results of the experimental program and model parameters

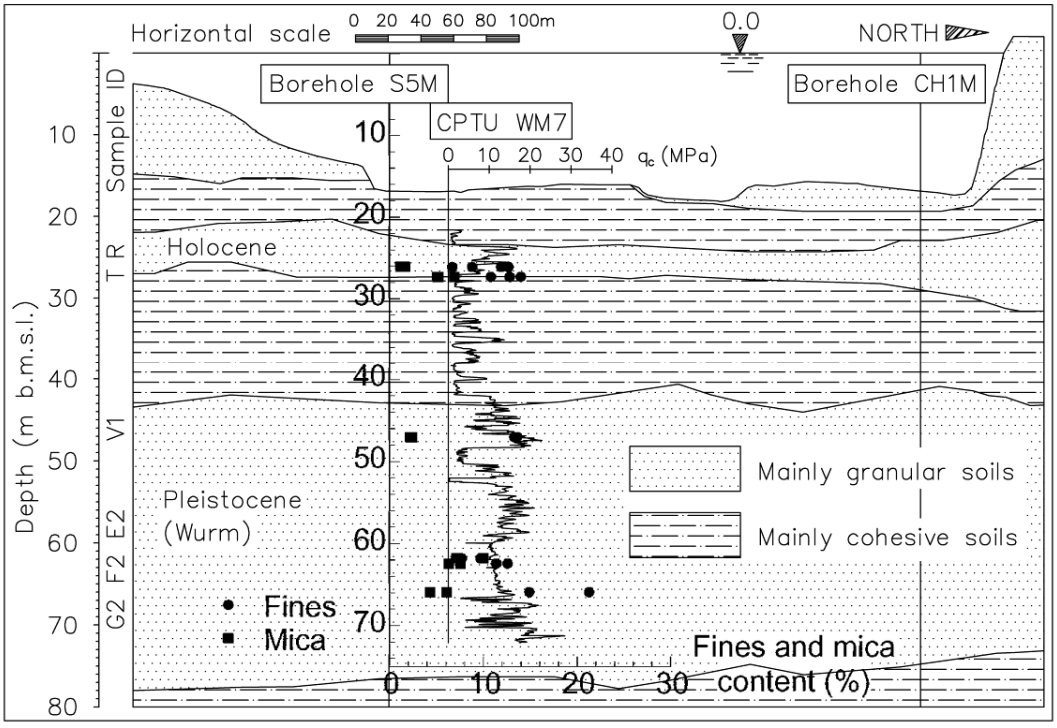

Figure 1: Cross-sectional profile of sub-surface soils below Malamocco inlet (after Ricceri, 1997), and physical properties of tube samples from borehole S5M

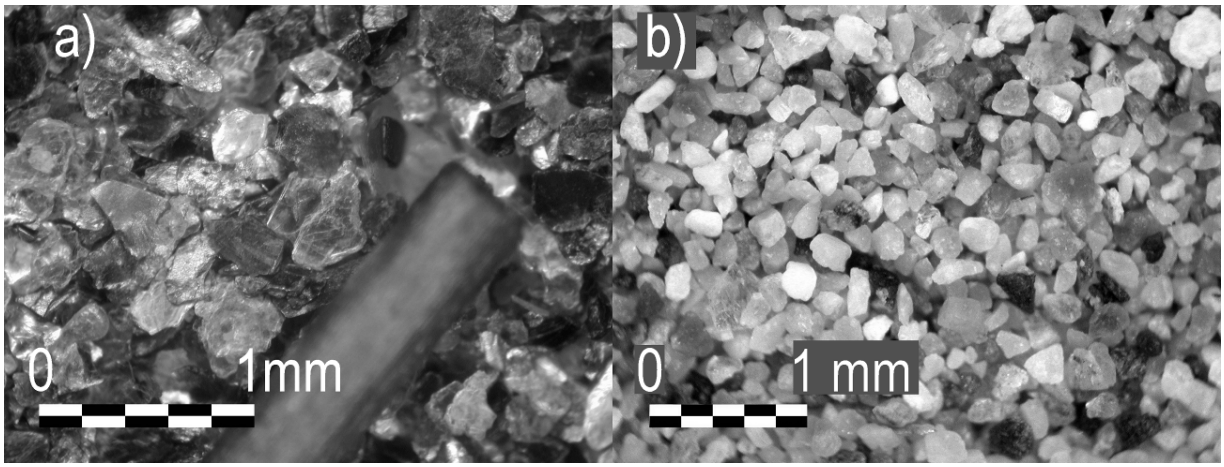

Figure 2: Separation of flat mica particles (a) and coarse sand fraction (b)

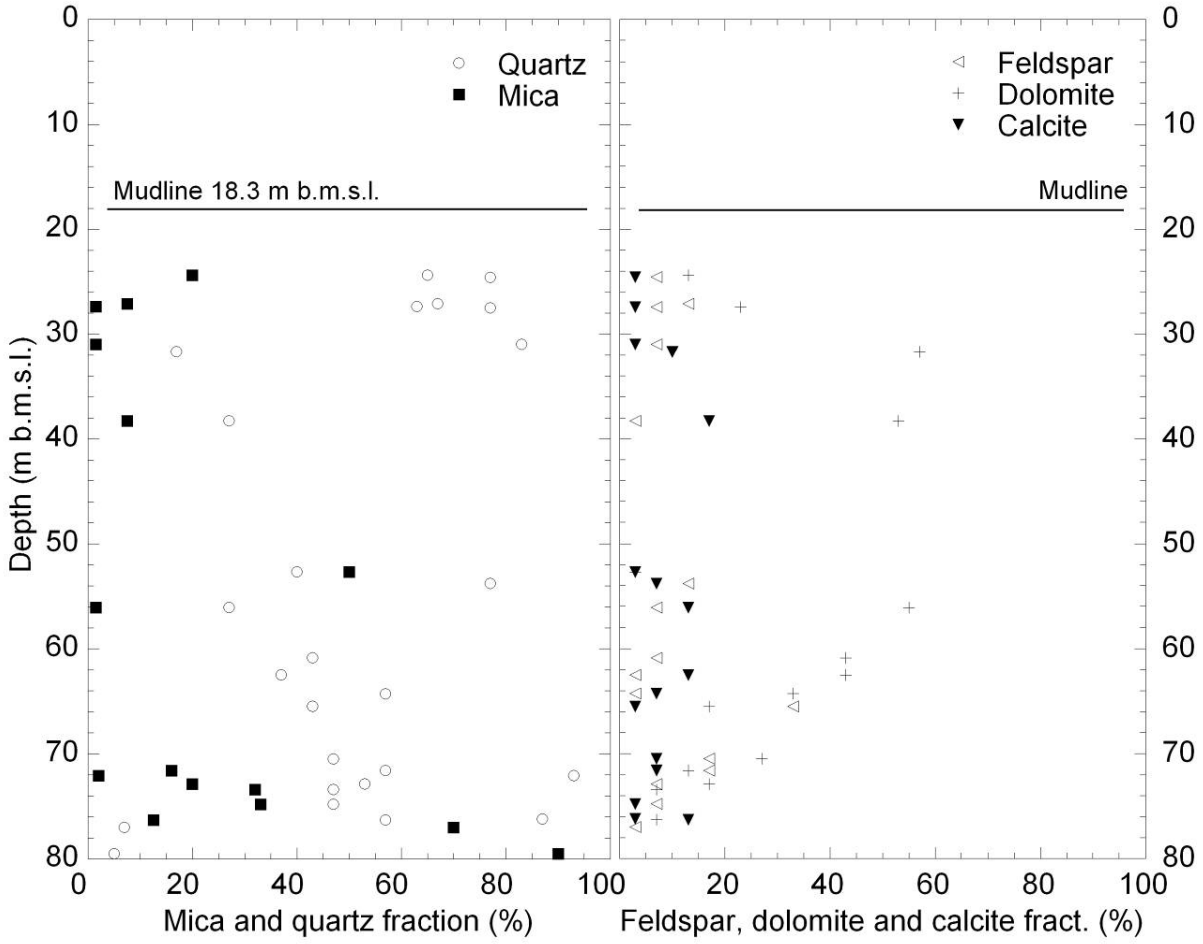

Figure 3: Mineralogical composition of Venice Lagoon sand, samples obtained from boring CH1M (Fontolan, 2005)

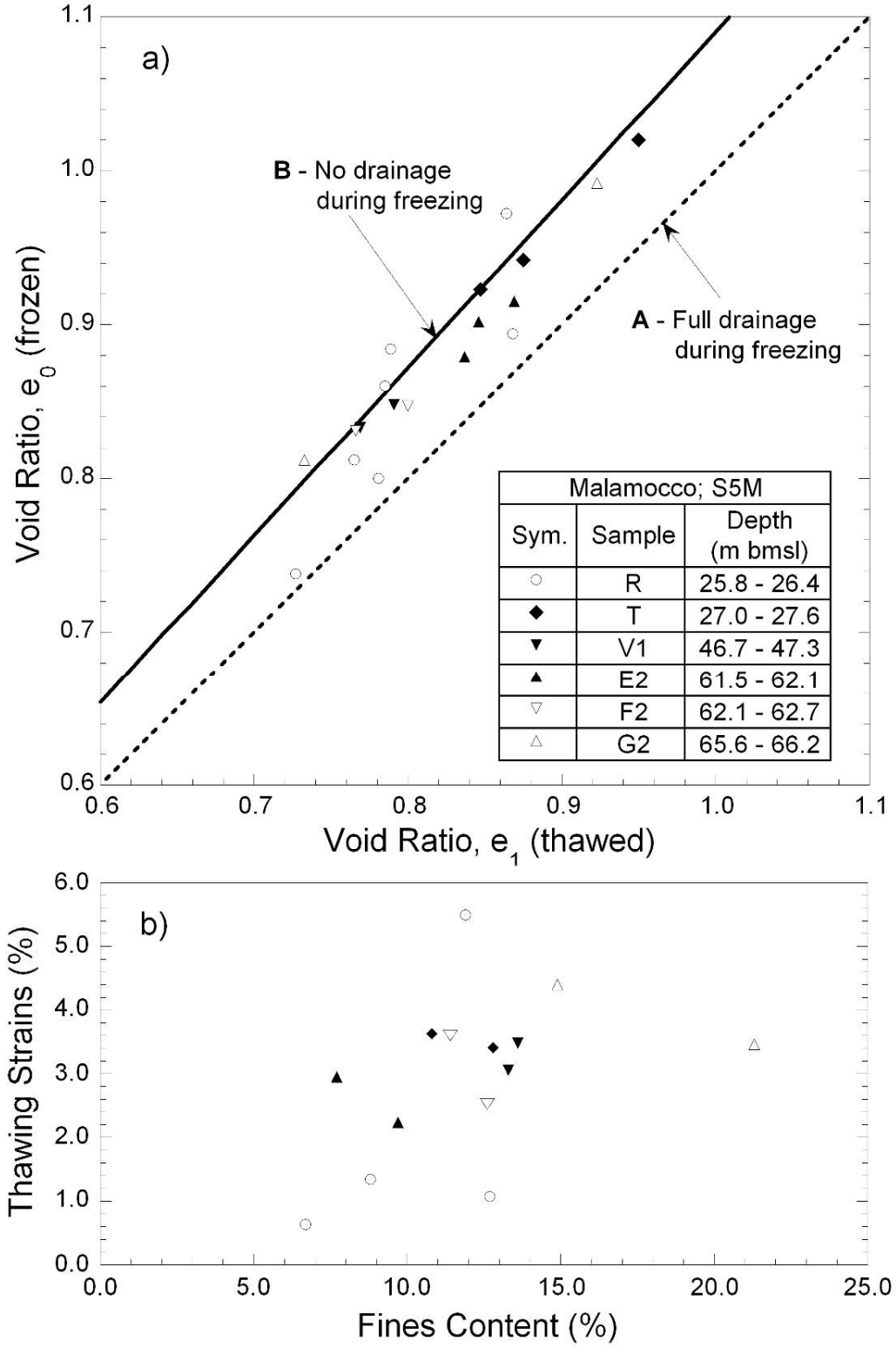

Figure 4: Comparison of void ratios for frozen and thawed intact sand specimens (a) and fines content versus thawing strains (b)

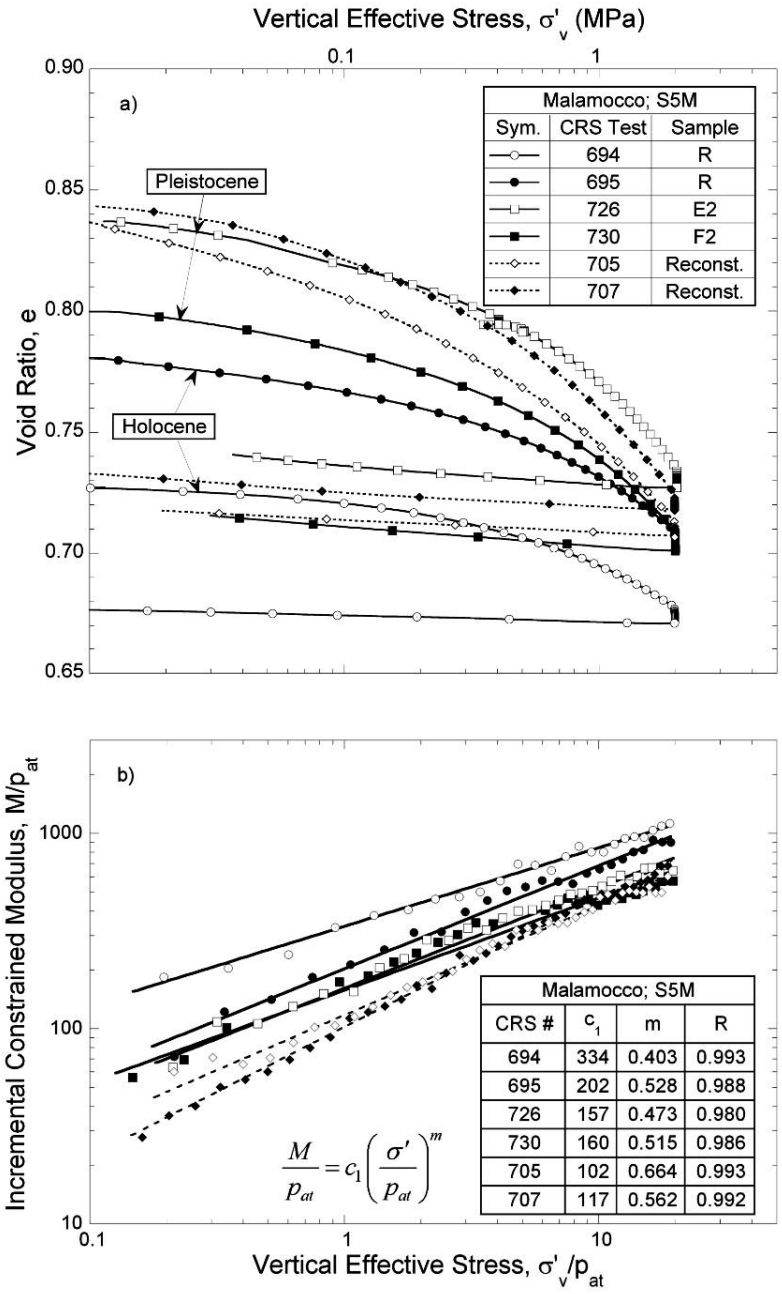

Figure 5: Compression behavior of intact and reconstituted specimens from the Malamocco Inlet: a) void ratio versus logσ'_v space; b) power law representation of 1-D constrained modulus, M

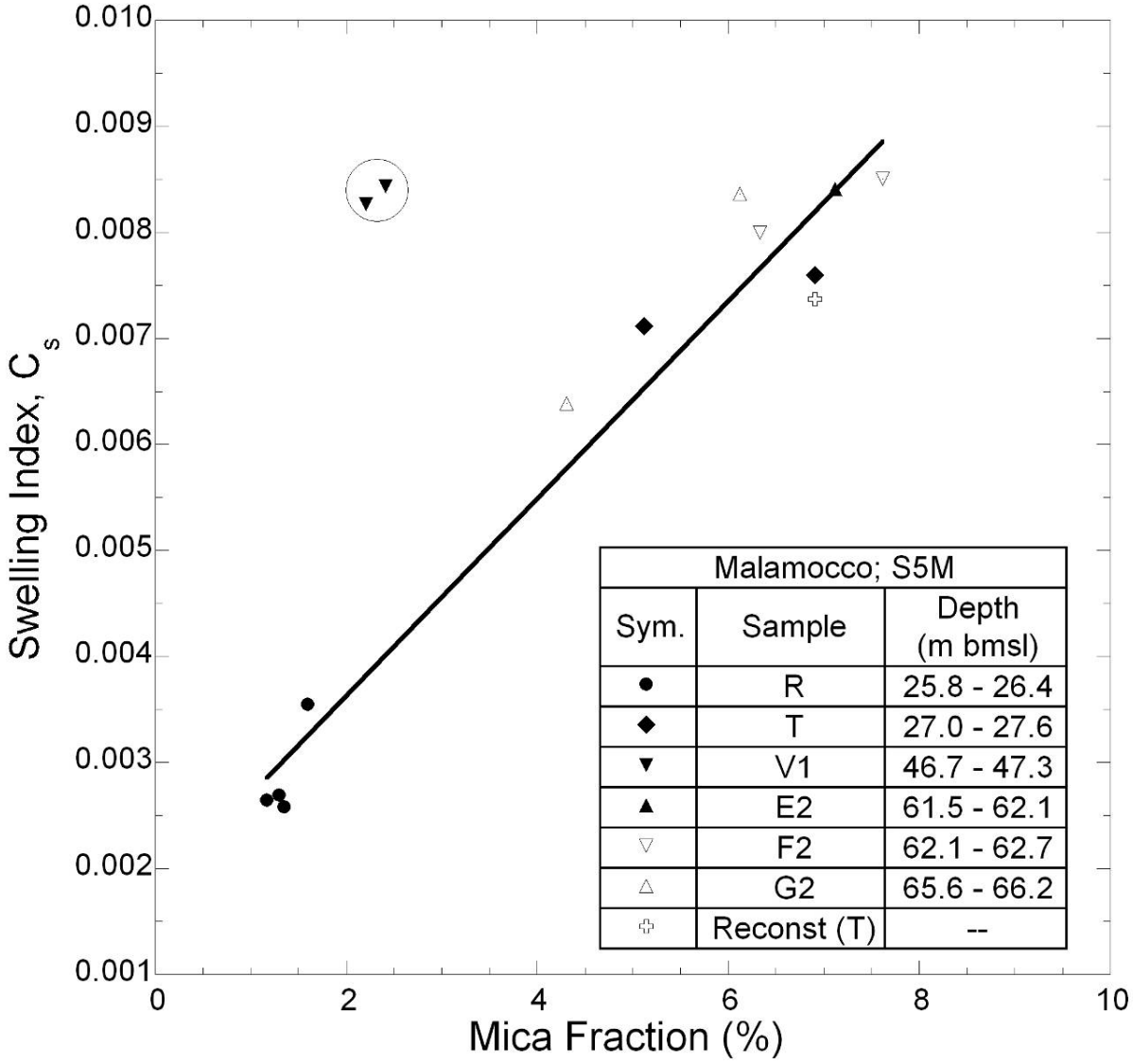

Figure 6: Correlation between mica content and swelling index

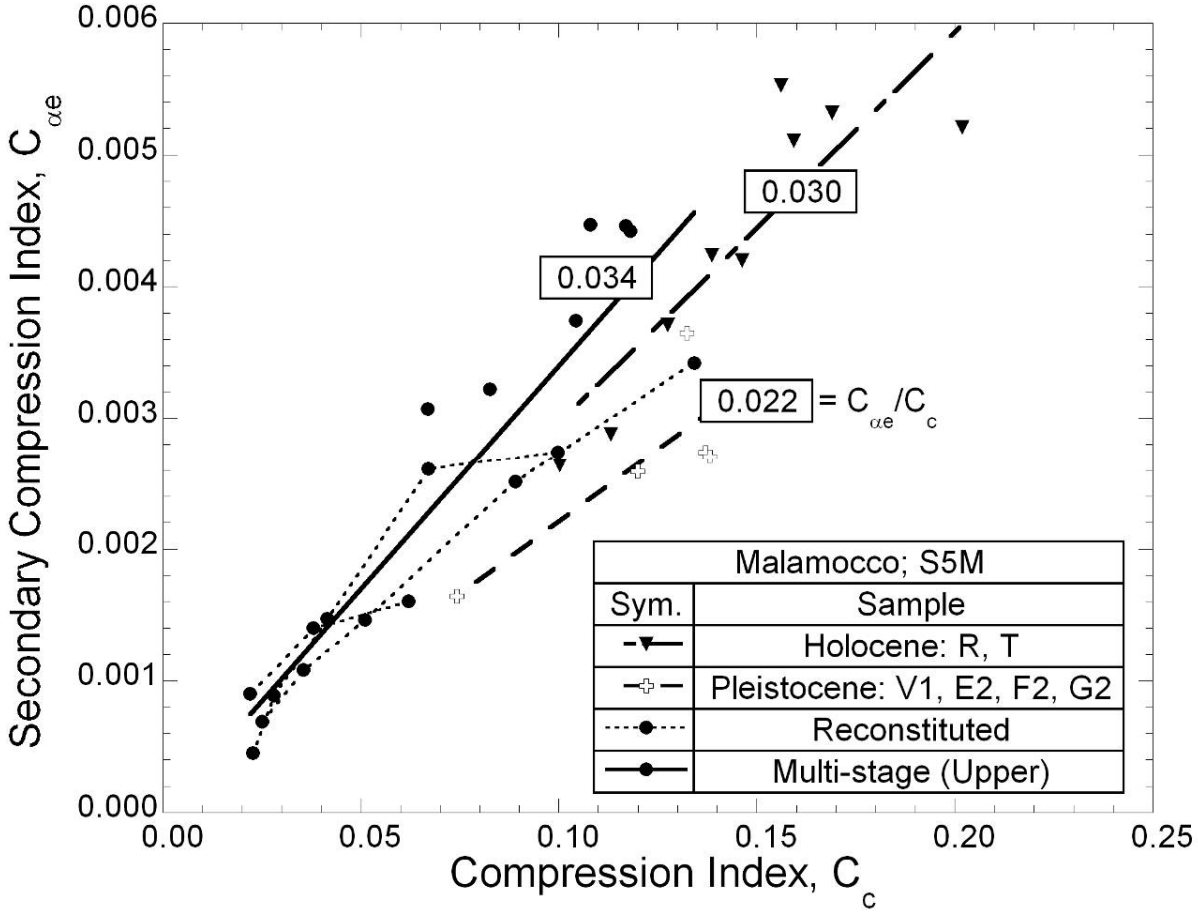

Figure 7: Correlation between compression index and secondary compression index

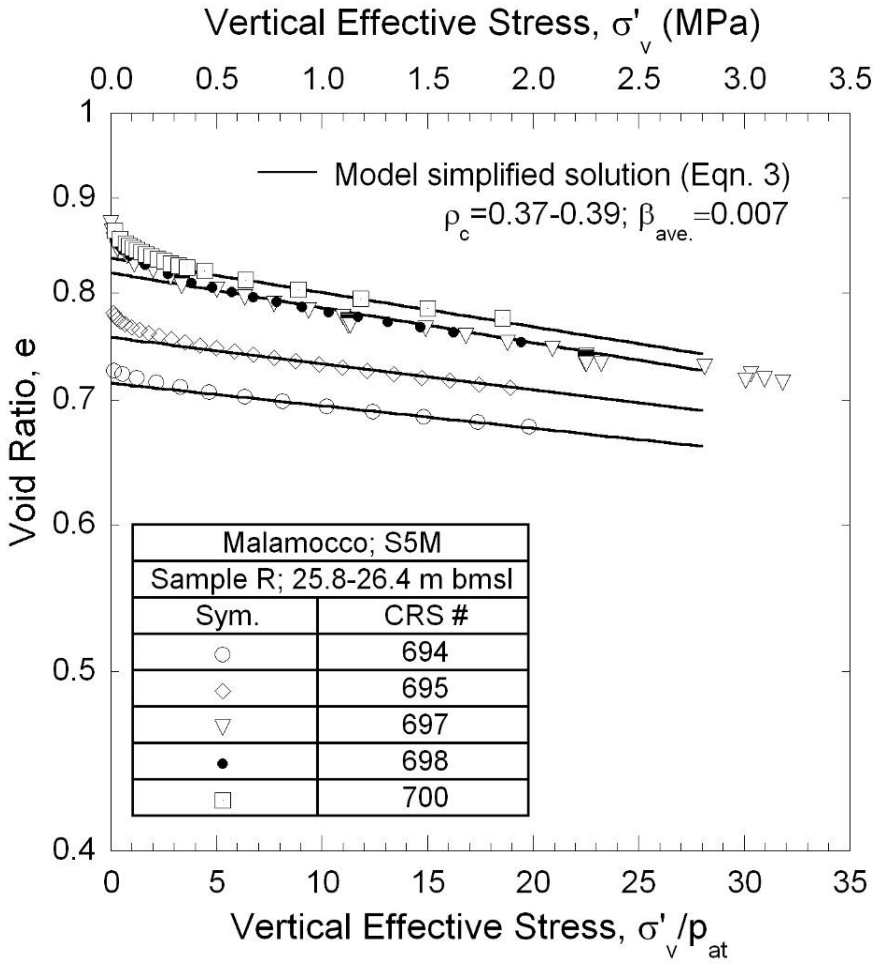

Figure 8: Comparison of measured data and simplified analytical solution (Eqn. 3a)

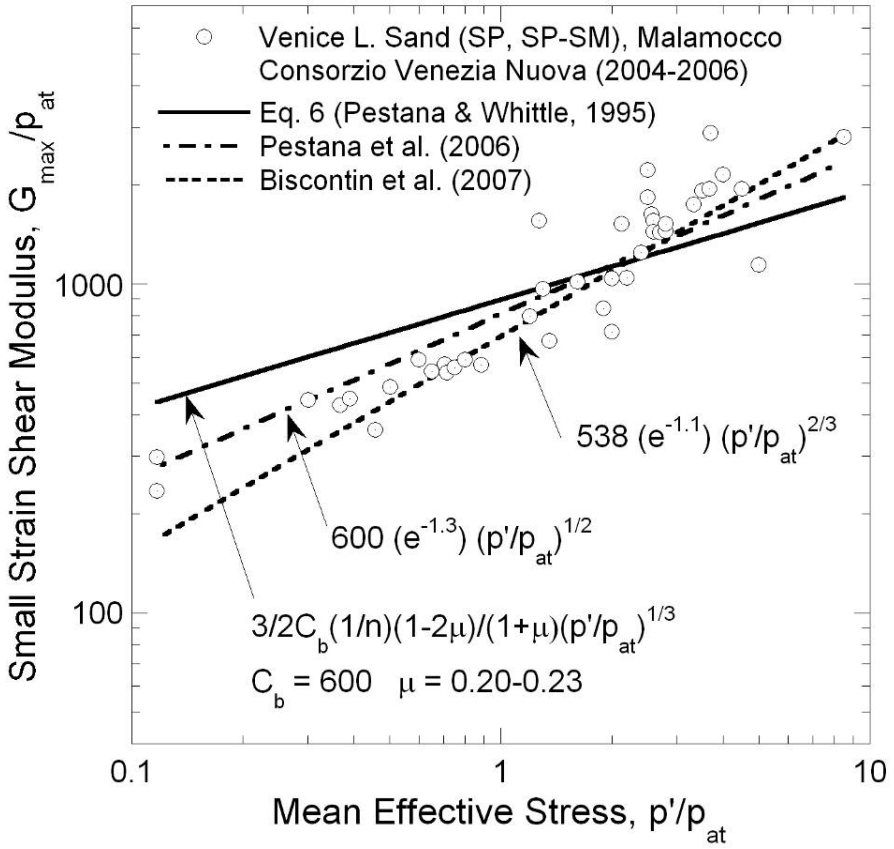

Figure 9: Comparison between measurements of shear modulus G_{max} and small strain stiffness relations

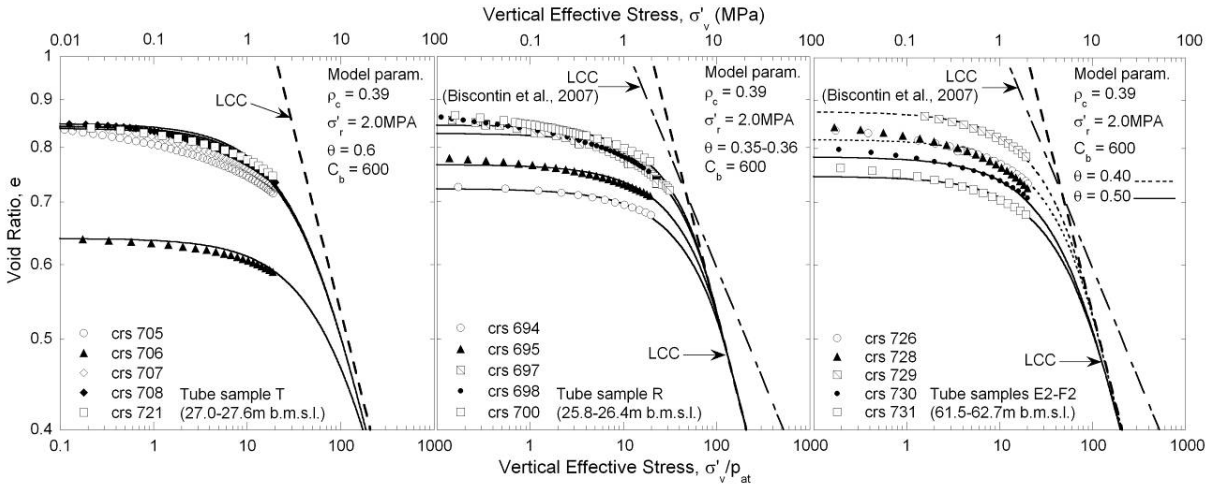

Figure 10: Evaluation of model compression parameters, reconstituted specimens (tube sample T, 27.0-27.6 m b.m.s.l.), upper Holocene intact specimens (R, 25.8-26.4 m b.m.s.l.), lower Pleistocene unit (E2-F2, 61.5-62.7 m b.m.s.l.)

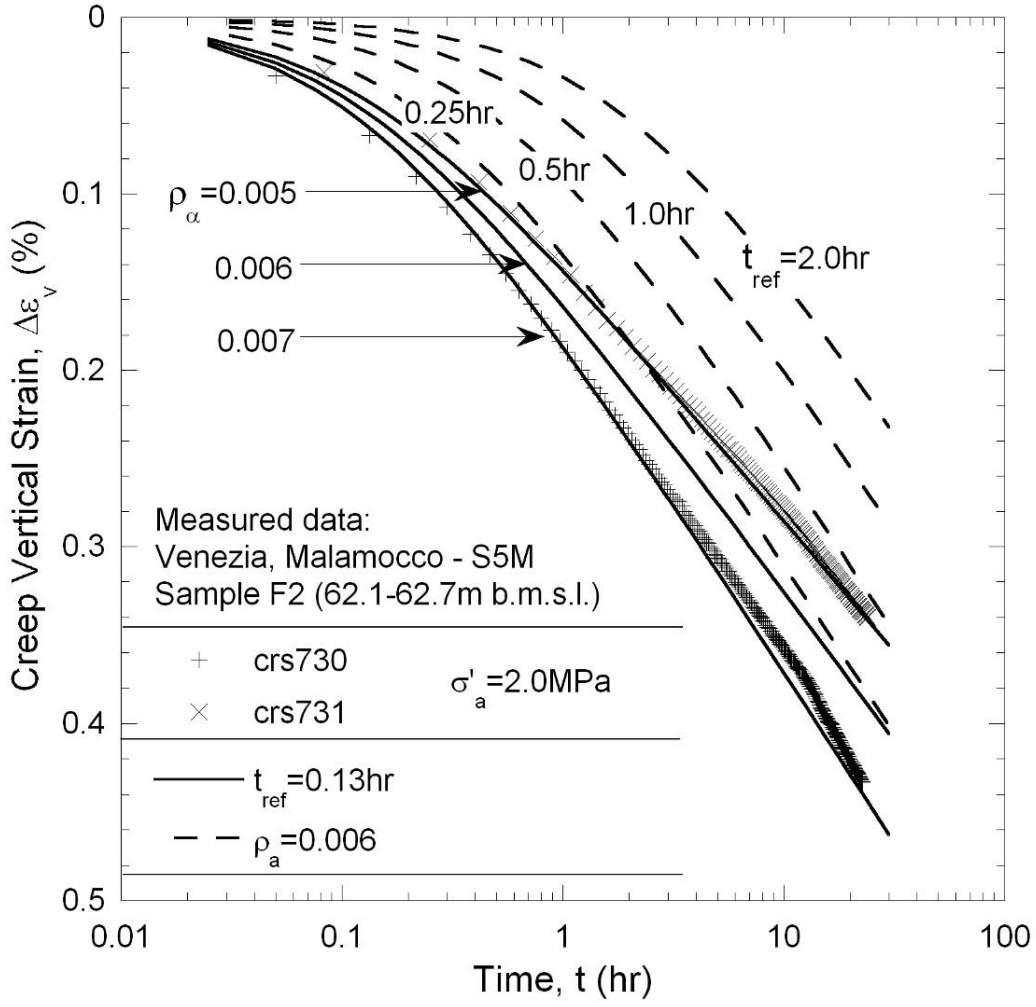

Figure 11: Selection of creep parameters t_{ref} and ρ_α

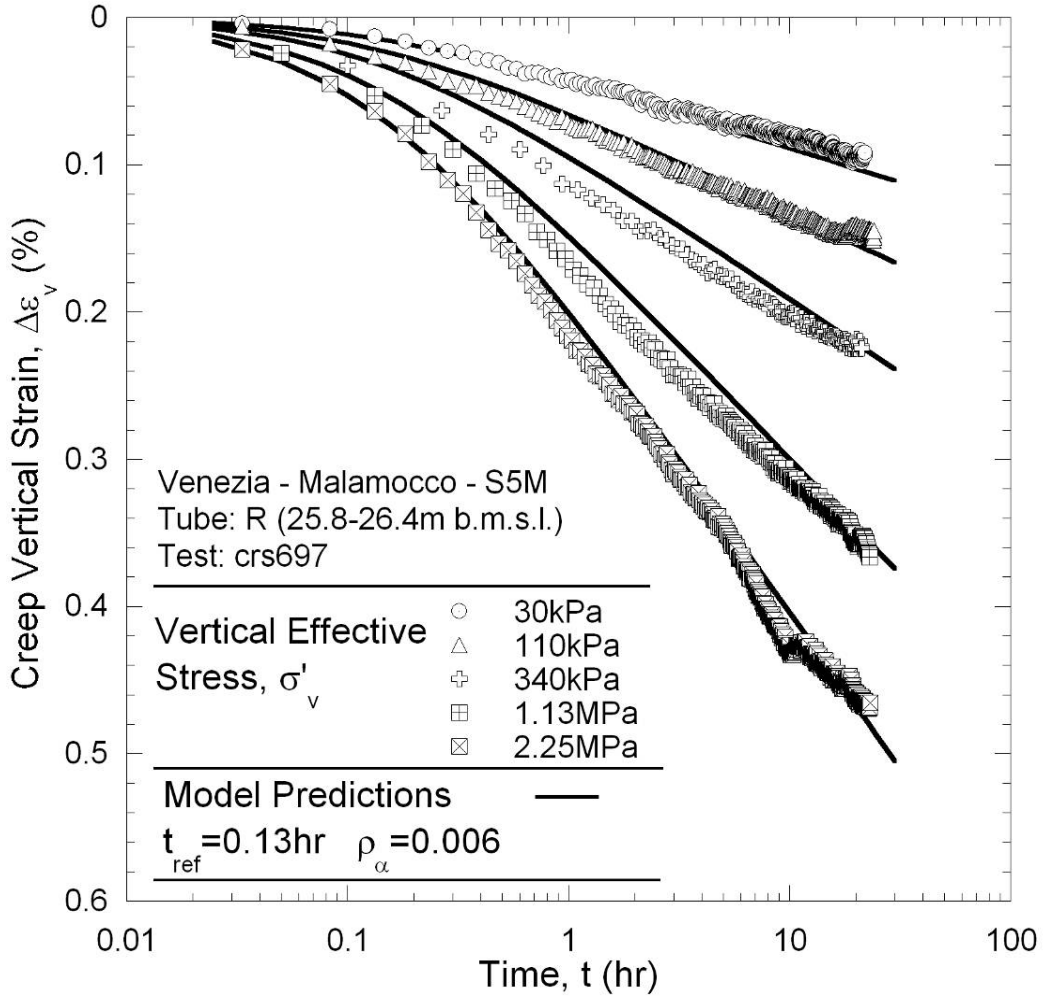

Figure 12: Comparison between measured data and model prediction of creep strain, sample R (25.8-26.4m b.m.s.l.)